ACOUSTICAL ANALYSIS OF ENCLOSURE DESIGN PARAMETERS FOR MICROSPEAKER SYSTEM

J. R. Chang* **C. N. Wang**

Department of Engineering Science and Ocean Engineering
National Taiwan University
Taipei, Taiwan

ABSTRACT

Microspeakers are key components of mobile devices in current consumer products; moreover, the user experience of multimedia products plays an essential role. The objective of this study was to investigate the acoustic performance of microspeakers in different enclosure parameters for mobile devices. Two methodologies are performed. The first model is an electro-mechano-acoustical model (EMA) of microspeaker along with distribution model of enclosure effect; the 2nd model, the details of diaphragms are taken into account in calculating the distribution models of microspeaker with enclosure parameters. They were combined and applied to determine microspeaker performance levels for mobile devices. Two methodologies show acceptable agreement with experimental results. The distribution model can well simulate the high frequency response than lumped model of microspeaker. The results can predict microspeaker system performance before industrial design and mechanism placement processes are executed.

Keywords: EMA, Microspeaker, Enclosure parameters, Distribution model.

1. INTRODUCTION

Miniaturization is the trend for computer, communication, and consumer electronics (3C) portable devices, such as mobile phones, personal digital assistants (PDAs), tablets, detachable devices and MP3 players. The loudspeakers in such devices are required to play speech and music signals with acceptable loudness and sound quality; the sound quality depends on the system frequency response. This poses a difficult problem in the design of microspeakers, whose physical sizes are typically compact. In contrast to large loudspeakers, the structures of microspeakers are typically simplified by removing the suspension and dome. The diaphragm serves as a sound radiator as well as the suspension.

Space is always limited in portable devices, and installing a loudspeaker in such a limited space is difficult. Therefore, determining how to produce a high-quality miniature loudspeaker that fits the space requirements of portable devices is imperative. Loudspeakers have been developed for more than 130 years [1-5]. Thiele and Small [6-14] have conducted a series of studies involving performance analyses of direct radiation loudspeakers, closed-box enclosures, and vented-box enclosures [6-14]. They have also developed a method for measuring the characteristic parameters, of a loudspeaker; such parameters are denoted as Thiele-Small (TS) parameters. Nearly all current loudspeaker designs are based on the research results of Thiele and Small. However, most developments were focused on large loudspeakers. Recently, miniature loudspeakers that are widely used in 3C products have received attention. The radiation pressure of microspeakers is low because of their small size. Determining how to increase the output pressure as well as evaluating how to extend the range of the frequency response have become the most crucial topics in the loudspeaker industry. Bai and Liao [15] used TS parameters and electro-mechano-acoustical (EMA) concepts to analyze and design miniature loudspeakers for mobile phones, and Bai *et al.* [16, 17] have optimized the design of a microspeaker [15-17] Shiah *et al.* [18] used TS parameters to simulate enclosure effects, front covers, and other factors affecting microspeakers [18]. Using the EMA approach to simulate loudspeaker performance is a lumped model, and the displacement of a loudspeaker is assumed to be the positon velocity; therefore, the radiation modes of a diaphragm cannot be fully investigated.

In this study, we applied two methodologies to predict acoustical system performance of microspeaker with different design parameters and to identify the accuracy for two methodologies. Two methodologies can cover a broad range of possibilities for mobile devices. Six cases were studied in simulations and experiments. The

* Corresponding author (meibus@yahoo.com.tw)

DOI : 10.1017/jmech.2017.64
Copyright © 2017 The Society of Theoretical and Applied Mechanics
https://doi.org/10.1017/jmech.2017.64 Published online by Cambridge University Press

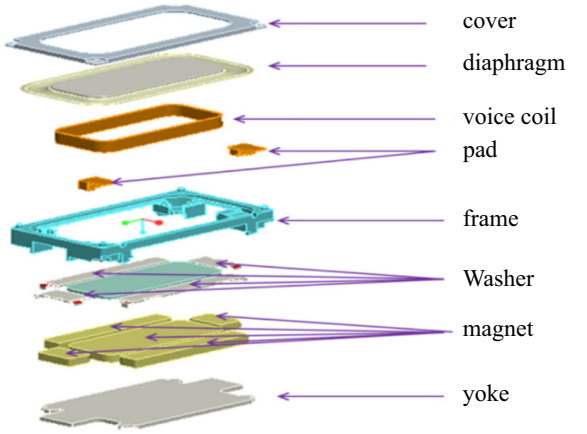


Fig. 1 Exploded view of a rectangular microspeaker (9 mm × 16 mm × 3 mm).

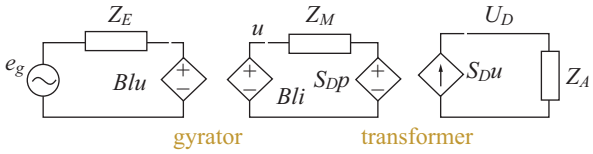


Fig. 2 Electro-mechano-acoustic analogous circuits.

simulation results highly agreed with experimental results. Especially, distribution mode of whole system simulation is precise than lumped model with distribution mode of enclosure parameters.

2. MODEL OF MICROSPEAKER WITH ENCLSOURE DESIGN PARAMETERS

In this paper, we consider the most frequently used rectangular microspeaker, with dimensions of 9 mm × 16 mm × 3 mm, in addition to comprising five magnets. A cross-sectional sketch of a typical direct-radiator microspeaker is shown in Fig. 1. The diaphragm is suspended by a cone, and it is made of polyetheretherkerketone with aluminum, which is supported at the outer edge and near the voice coil to ensure that, it is free to move only in an axial direction.

2.1 EMA Analogous Circuit of Microspeaker with Finite-Element Analysis of Enclosure Design Parameters

Part of the EMA analogous circuit was used to model the microspeaker system in COMSOL Multiphysics software, in which all variables of the electrical, mechanical, and acoustical domains can be analyzed with a unified framework. Figure 2 shows the EMA analogous circuit used for moving dynamic loudspeakers. The dynamics of each subsystem are lumped into a single impedance element. The coupling of the electrical domain and mechanical domain was modeled by a gyrator, with the mechanical system being represented by the impedance analogy, whereas the coupling of the mechanical domain and acoustical domain was modeled by a transformer. Figure 3 presents an exploded view of the impedance elements in the electrical system and mechanical system, where the mechanical system was modeled by a simple resonator. The impedance of the acoustical system is discussed in more detail to demonstrate our differentiation model. The advantage of using the EMA analogous circuit is that the coupled systems can be analyzed using common techniques applied for evaluating electric circuits. The steady-state and transient responses can be predicted readily with the aid of equivalent circuits. The electrical system is mainly the voice coil that can be modeled as an inductor L_E and a resistor R_E whose electrical impedance is written as

$$Z_E = R_E + j\omega L_E \tag{1}$$

The mechanical system comprising the diaphragm, the voice coil, and the suspension is modeled as a second-order system with the following mechanical impedance:

$$Z_M = j\omega L_E + R_{MS} + \frac{1}{j\omega C_{MS}} \tag{2}$$

The impedance of the acoustical system is more complex than those of the other two subsystems and is attributed to effects from cavities, ducts, perforations, and radiation loading associated with the mobile enclosure. Here, it can be simplified by lumping acoustical impedances together into two terms, from the front (Z_{AF}) and the back (Z_{AB}) of a microspeaker with a system enclosure,

$$Z_A = Z_{AF} + Z_{AB} \tag{3}$$

The coupling of the electrical domain and mechanical domain is represented by a gyrator that follows two electrodynamical laws,

$$f = Bli \tag{4}$$

$$e = Blu \tag{5}$$

where i is the current flowing in the voice coil, e is the voltage induced by coil motion across the voice-coil terminals, f is the Lorentz force produced by the current, and u is the cone velocity of the diaphragm. Two basic variables in the acoustical domain are pressure P and volume velocity U. The coupling of the mechanical domain and acoustical domain can be simulated by a transformer, according to the following relations between P and U:

$$f = S_D P \tag{6}$$

$$U = S_D u \tag{7}$$

The volume velocity U emitted by a source is the time derivative of the volume of air it displaces. Consider a

https://doi.org/10.1017/jmech.2017.64 Published online by Cambridge University Press

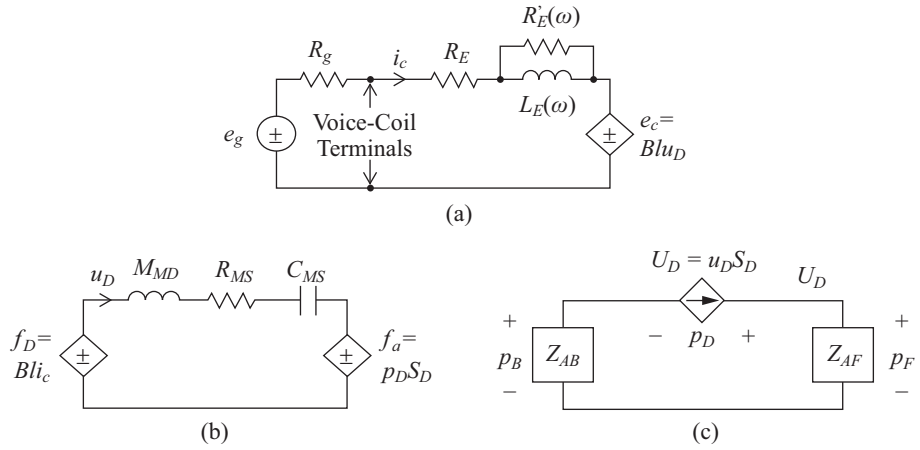


Fig. 3 Impedance of electro-mechano-acoustic analogous circuits.

Table 1 Microspeaker parameters.

Electrical Parameters			1	2	3	4	5	6	7	8	9	10	AVG
Re	Electrical voice coil resistance at DC	Ohm	5.96	5.93	5.98	5.99	6	5.99	6.01	5.98	6.02	6.03	5.989
Le	Frequency independent part of voice coil inductance	mH	0.028	0.03	0.029	0.029	0.028	0.028	0.029	0.029	0.029	0.03	0.0289
Mechanical Parameters													
Mms	"Mechanical mass of driver diaphragm assembly including air load and voice coil"	g	0.06	0.061	0.06	0.061	0.06	0.064	0.058	0.055	0.059	0.056	0.0594
Rms	Mechanical resistance of total-driver losses	kg/s	0.07	0.064	0.066	0.073	0.063	0.068	0.061	0.057	0.06	0.053	0.0635
Cms	Mechanical compliance of driver suspension	mm/N	1.904	1.759	2.13	1.943	1.899	1.875	1.77	2.128	1.975	2.103	1.9486
Kms	Mechanical stiffness of driver suspension	N/mm	0.53	0.57	0.47	0.51	0.53	0.53	0.57	0.47	0.51	0.48	0.517
Bl	Force factor (Bl product)	N/A	0.643	0.64	0.635	0.627	0.623	0.633	0.622	0.609	0.632	0.62	0.6284
Other Parameters													
Vas	Equivalent air volume of suspension	1	0.0024	0.0022	0.0027	0.0025	0.0024	0.0024	0.0023	0.0027	0.0025	0.0027	0.00248
Sd	Diaphragm area	cm^2	0.95	0.95	0.95	0.95	0.95	0.95	0.95	0.95	0.95	0.95	0.95

microspeaker mounted in a closed-box with the parameters shown in Table 1. Let S_D, X_D and U_D denote the diaphragm piston area, displacement, and velocity respectively. The volume of air displaced is $V = S_D x$. The volume velocity emitted is Eq. (7). The equivalent piston area of a diaphragm is defined as the area of a flat piston that emits the same volume velocity. The rule states that the piston radius in centimeters is equal to the documented diameter. The phase volume velocity emitted is given by

$$U = 4\pi r^2 u_r(r) = 4\pi r^2 \frac{P(r)}{Z_s} = \frac{4\pi K}{j\omega\rho}\left[1 + j\frac{\omega r}{c}\right]\exp(-jkr) \tag{8}$$

After the network has been solved for the required volume velocities, the far-field acoustic pressure P can be calculated by assuming that the system behaves as a point source.

$$P = j\frac{\rho c k}{2\pi r} U S_D Exp\ j(\omega t - kr) \tag{9}$$

where ρ is the density of air
c is the velocity of sound in air
ω is the angular frequency (where $\omega = kc$)
k is the wavenumber (where $k = 2\pi/\lambda$)
r is the distance from the source to the observation point

The on-axis pressure radiated is defined by Eq. (9). The sound pressure level, (SPL) is defined by

$$SPL = 20\log\left(\frac{P}{P_r}\right) \tag{10}$$

where $P_{ref} = 2\times10^{-5}\,Pa$

According to the preceding theory, this paper presents a new methodology for predicting the microspeaker system frequency response with the enclosure parameters, as illustrated by the new schematic in Fig. 4. The acoustic module of COMSOL Multiphysics software is employed instead of an acoustic circuit in the acoustical domain by using the finite element method. Before implementing the simulation, we investigated the lump parameters of the microspeaker through klippel system to

https://doi.org/10.1017/jmech.2017.64 Published online by Cambridge University Press

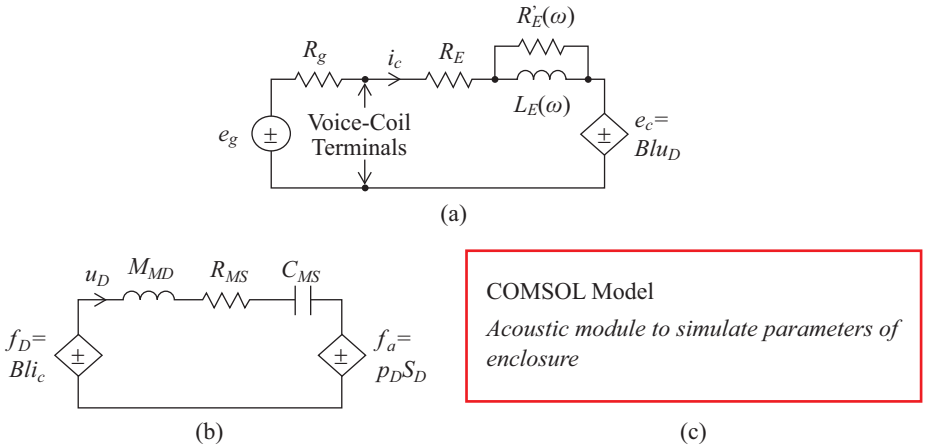


Fig. 4 Hybrid model of the microspeaker with parameters of enclosure.

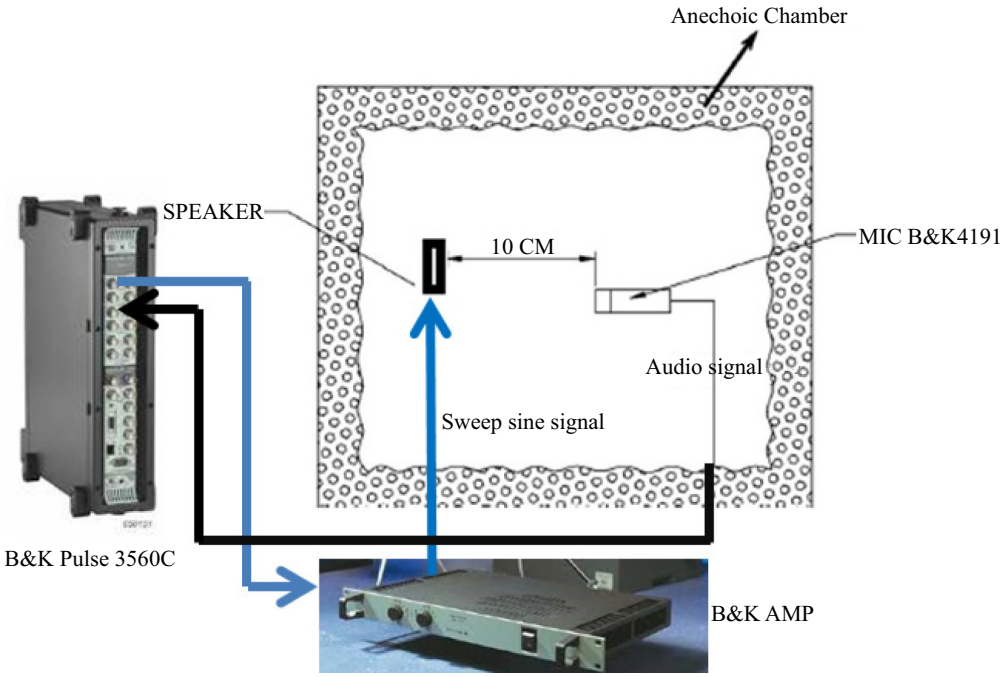


Fig. 5 Measurement setup.

acquire TS parameters under a small signal with 0.1 Vrms. To the accuracy of TS parameters, we evaluated 10 samples and averaged the results. The TS parameters are present in Table 1. Those parameters were set in our model to produce a uniform positon velocity; the acoustic domain of the microspeaker and the enclosure parameters were simulated by the COMSOL finite-element. To measure the sound pressure response of a microspeaker system, B&K PULSE Electroacoustics system in addition to sound check software, and a highly sensitive microphone (B&K Type 4191) were used to record the sound pressure response of the microspeaker system in an anechoic chamber. The frequency range from 100 Hz to 20 KHz of the microspeaker is measured using 0.1 Vrms sweep sine input. A schematic of the experimental apparatus is shown in Fig. 5. Figure 5 shows the experimental arrangement for measuring the on-axis *SPL* response by using a microphone positioned at 5 cm away from the microspeaker system.

2.2 Finite-Element Analysis of Microspeaker with Enclosure Design Parameters

The displacement of the diaphragm under an electromagnetic force load was calculated by using the finite element method. First, the diaphragm and coil were discretized with elements and the force equations on each node were established. The combined equations in matrix form are expressed as

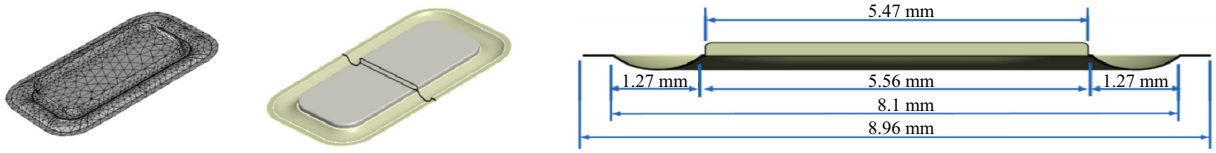
$$[M]\{\ddot{x}(t)\}+[c]\{\dot{x}(t)\}+[K]\{x(t)\}=\{F(t)\} \qquad (11)$$

where $[M]$, $[c]$, and $[K]$ are the mass, damping, and stiffness matrices, respectively; and represents the displace-

https://doi.org/10.1017/jmech.2017.64 Published online by Cambridge University Press

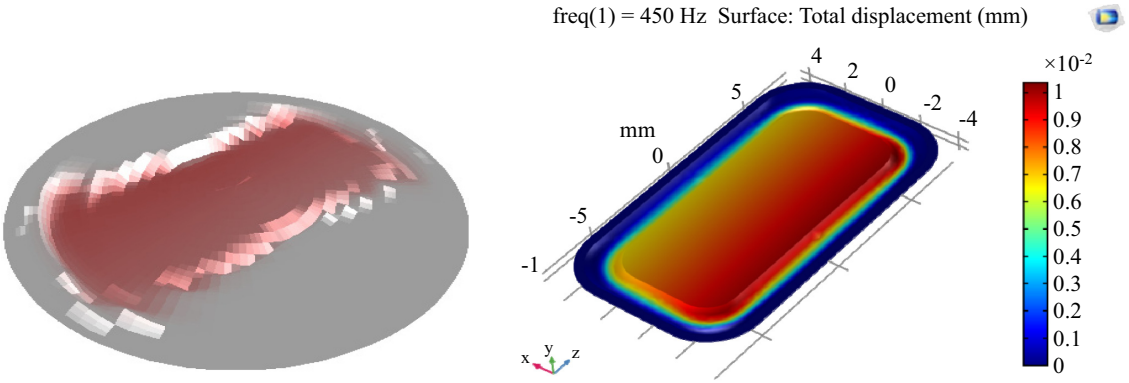
Table 2 Material properties of the diaphragm and voice coil assembly.

	Young's modulus	Poisson's ratio	Density
Dome	10 [GPa]	0.3	503.8 [kg/m^3]
Surrounding	0.9 [GPa]	0.3	3963.5 [kg/m^3]
Coil	110 [GPa]	0.35	5414.8 [kg/m^3]



(a) (b)

Fig. 6 Schematic diagrams of the diaphragm and voice coil of the microspeaker. (a) top view. (b) Cross section.



(a) (b)

Fig. 7 Modal shapes of diaphragm-voice coil assembly obtained using the FEA and measurement. (a) Klippel measurement. (b) The first position mode.

ment vector of all nodes. All the material properties for the diaphragm required in the calculation are given in the Table 2. In order to obtain the characteristic frequencies and normal modes, the damping force and the applied load terms are not considered. Assume the displacement is expressed as $\{x(t)\} = \{\phi\}e^{i\omega t}$, Eq. (11) can be rewritten as

$$\{[K]-\omega^2[M]\}\{\phi\} = \{0\} \tag{12}$$

Using the software COMSOL Multiphysic, the characteristic frequencies of each mode are achieved by

$$|[K]-\omega^2[M]| = 0 \tag{13}$$

Consequently the normal mode shapes can also be obtained by Eq. (12). Furthermore, using Eq. (11), the displacement of each node can also be calculated when the force is applied. The radiated sound pressure was calculated using the Rayleigh integral and is expressed as

$$p(\omega,\alpha) = j\frac{\omega^2\rho_0}{2\pi}\int_{S_c}\frac{X(\omega,\beta)}{|\alpha-\beta|}e^{-jk|\alpha-\beta|}dS_c(\beta) \tag{14}$$

where ρ_0 is the density of media, ω is the angular frequency, S_c denotes the diaphragm area, α is the observing point, β is the point on the diaphragm, and X represents the displacement amplitude at point β. Therefore, the frequency response of a loudspeaker can be obtained by numerical integration when the surface of the diaphragm is discretized.

The FEA is applied to model the diaphragm-voice coil assembly shown in Figs. 6(a)-(b), the material properties of the diaphragm-voice coil assembly are included in Table 2. The FEA is conducted using COMSOL Multiphysic, where the element "shell 63" is used. The finite-element model and the mesh of diaphragm with voice-coil are shown in Fig. 6(a). The boundary conditions are selected that all degrees of freedom for the outer rim of the diaphragm and the X, Y-displacements of the voice-coil are set to zero. The fundamental resonance frequency calculated by the modal analysis is 450 Hz and the associated mode shape is shown in Figs. 7(a)-(b). The fundamental mode known as the position mode can be used to "finite-tune" FEA parameters to match the measurement data. The complex displacements calculated using the FEA harmonic analysis is

https://doi.org/10.1017/jmech.2017.64 Published online by Cambridge University Press

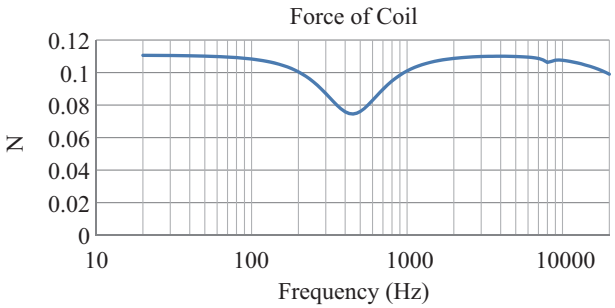


Fig. 8 Short-circuit mechanical impedance of the diaphragm-voice coil.

Table 3 Design parameters

	Item	Parameters	Reference Picture
Case 1	Front open ratio (100%)	Rear volume: 0.1cc, 0.6cc, 1cc.	Fig. 9(a)
Case 2	Rear volume is 1cc	Front open rate: 100%, 60%, 40%,	Fig. 9(b)
Case 3	1. Front open ratio (50%) 2. Rear volume (1cc)	Front chamber volume: 0.1cc, 0.5cc, 1cc,	Fig. 9(c)
Case 4	1. Front open ratio (100%) 2. Rear volume (1cc)	Front chamber volume: 0.1cc, 0.5cc, 1cc,	Fig. 9(d)
Case 5	1. Front open ratio (50%) 2. Rear volume (1cc)	In middle location, shift 50%, shift 100%	Fig. 9(e)
Case 6	1. Side firing 2. Rear volume (1cc)	1. Channel high is 1mm, channel length is 5mm, open area is 16sq mm. 2. Channel high is 1mm, channel length is 10mm, open area is 16sq mm. 3. Channel high is 2mm, channel length is 5mm, open area is 32sq mm. 4. Channel high is 2mm, channel length is10mm, open area is 32sq mm.	Fig. 9(f) Fig. 9(g)

then converted into the average velocity (U). Using (4), the mechanical impedance of the diaphragm-voice coil assembly can be calculated, as shown in Fig. 8. As a result, the dynamics of the flexible diaphragm is represented by a frequency-dependent impedance element and is readily integrated into the destitution model.

3. PARAMETRIC INVESTIGATATION

Mobile devices have many display sizes. Moreover, different form factors, are associated with different microspeaker system performance levels, rendering the task of predicting; the final performance is challenging.

As mentioned, the *SPL* response is actually a coupled output of various parameters. Each design parameter has a unique implication for *SPL* responses. The theory comparison of the lumped model with the distribution model of enclosure parameters and whole distribution model, as described in the preceding section, were conducted to enable achieving an *SPL* simulation that agreed with experiment conducted in both the low-frequency range and high-frequency range- of sounds audible to human ears. In the subsequent parametric experiments, we focused on qualitative research and quantitative research for output *SPL* of the six test cases shown in Table 3.

3.1 Case 1 Enclosure Effects

Generally, a microspeaker simultaneously produces sound not only from its front but also from its back. The phases of both sound sources are opposite, and consequently, the interference between them leads to the degradation of the overall sound pressure level and frequency response. For experiments in an anechoic chamber, a baffle may be installed to enable data collection from the front source only. Specifically, sound interference from the back of the microspeaker is usually blocked by an enclosure or a baffle-like structure.

To investigate the enclosure effect, three distinct back enclosure volumes, namely, 0.1, 0.6 and 1c.c, were considered. The enclosed air provides a compliance that also served to limit the low-frequency excursion of the driver unit, hence improving longevity. The resultant acoustic pressure output exhibited the property of a second-order high-pass filter, with the asymptotic roll-off

https://doi.org/10.1017/jmech.2017.64 Published online by Cambridge University Press

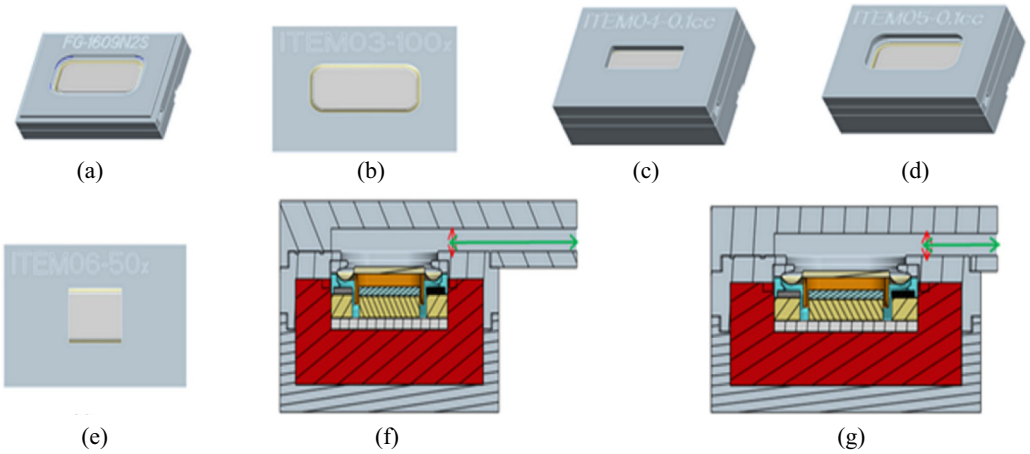


Fig. 9 (a) Case 1 (b) Case 2 (c) Case 3 (d) Case 4 (e) Case 5 (f) Case 6-1 (g) Case 6-2.

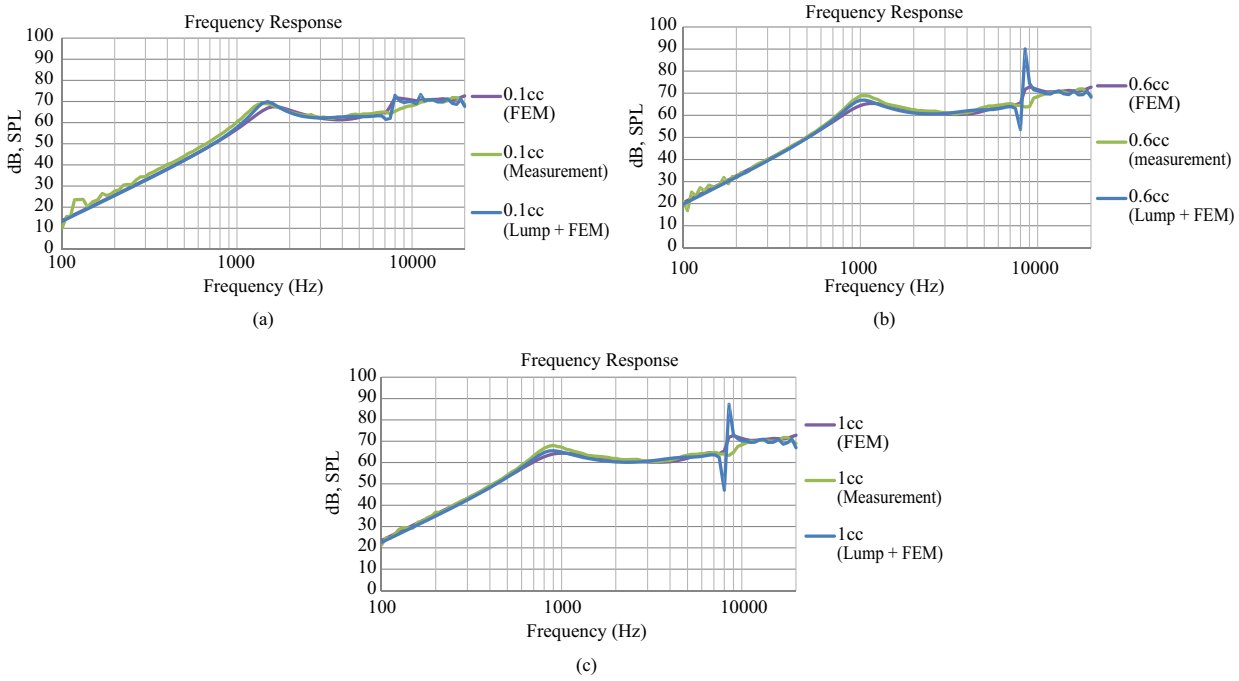


Fig. 10 Case 1 results, (a) Rear chamber = 0.1c.c. (b) Rear chamber = 0.6c.c. (c) Rear chamber = 1c.c.

being 12dB/octave (Fig. 10). Note that sealing the enclosure hermetically may be ill-advised; any changes in atmospheric pressure would cause changes in the equilibrium position of the driver. Figure 10, illustrates the normal closed-box design, indicating that the box is large and that the compliance of the enclosed air is high; the compliance of the driver unit itself is predominant, and the enclosure serves merely to isolate the rear radiation. However, in the acoustic suspension design, the enclosure was sufficiently small to exert a controlling influence on the effective compliance of the system. The front face of the driver was the only source of acoustic radiation; the required volume velocity was obtained easily from a calculation of V_d. In this case, both measurement results and simulation results showed excellent agreement, and because the large back chamber volume had high compliance, the box resonance frequency was low [Fig. 10(c)]. The box resonance frequency can be calculated by Eqs. (15) and (16):

$$\alpha = \frac{V_{as}}{V_B} \tag{15}$$

$$f_c = f_s\sqrt{1+\alpha} \tag{16}$$

where V_{as} is the equivalent air volume of suspension.
V_B is back chamber volume.
f_s is the resonance frequency of the microspeaker driver unit.
f_c is the resonance frequency of the microspeaker system.

In comparison of lumped model with distribution model of enclosure parameters and whole distribution

https://doi.org/10.1017/jmech.2017.64 Published online by Cambridge University Press

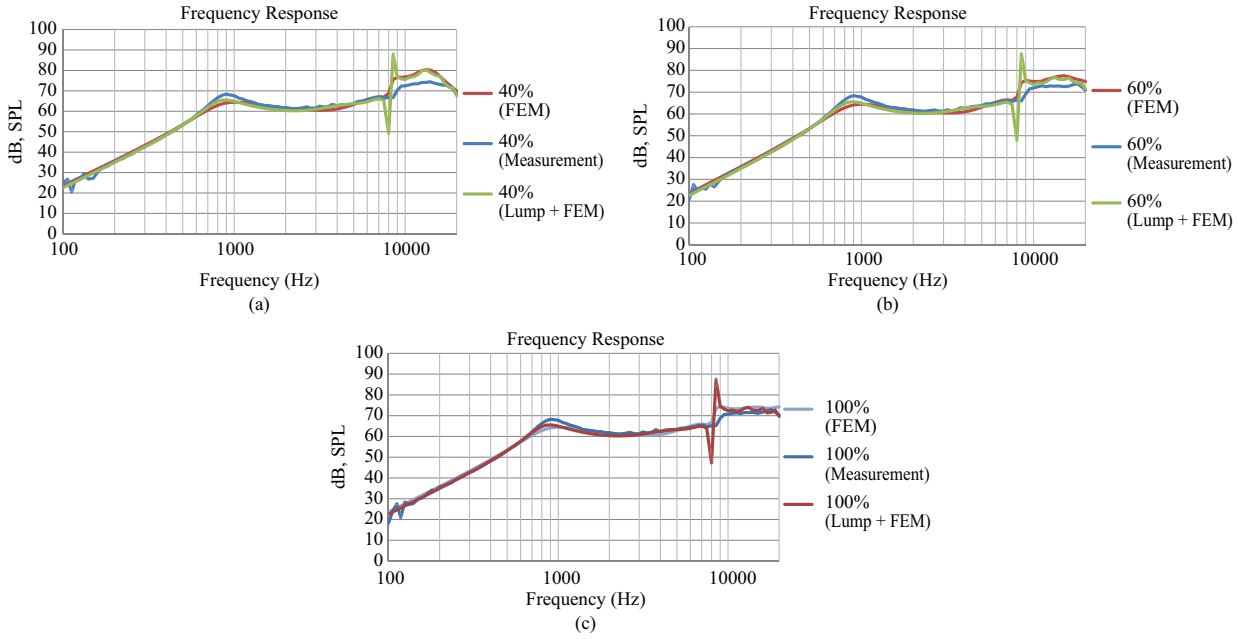


Fig. 11 Case 2 results, (a) 40% open rate; (b) 60% open rate; (c) 100% open rate.

model, both results got agreement with experiment in low frequency range, but the whole distribution model can provide more accuracy approach in high frequency range, because the mode shape of diaphragm in high frequency components can be calculated by finite-element method.

3.2 Case 2 Enclosures with Different Front Open Areas

Front chamber open rates have major effects on the *SPL* response of complete microspeaker driver units installed in mobile devices. As shown in Table 3, we investigated, three cases of front chamber open rates, with back chamber volume being maintained at 1cc. The microspeaker driver measured 16 mm × 9 mm × 3 mm; therefore, the whole open area of the microspeaker measured 16 mm × 9 mm. We examined the three cases to explain the effects on their *SPL* curves and cut-off frequency of the low-pass filter. The simulated and experimental *SPL* curves derived for the two cases are presented in Fig. 11. Comparing the simulated and measured *SPL* curves revealed that, both curves exhibited a consistent trend; specifically, increasing the open area (open rate) of the front chamber open port can facilitate reducing the rise-up effect of f_H. The results demonstrate that; an open area of 60% in our investigated model is large enough to yield an *SPL* response similar to that of the case with 100%. In comparison of lumped model with distribution model of enclosure parameters and whole distribution model, both results got agreement with experiment in low frequency range, but the whole distribution model can provide more accuracy approach in high frequency range, because the mode shape of diaphragm in high frequency components can be calculated by finite-element method. Based on the simulation and experiment, we found the physic symptom if open rate is over than 60%, the high frequency response will not be influenced. As long as open rate is less than 40%, the 2nd resonance frequency of enclosure is obvious.

3.3 Case 3 Enclosures with 50% Open Started with Different Chamber Volume

The case involving the 1 cc back chamber volume reveals that if an industrial design provides only a 50% open rate for a sound port, then the placement of microspeaker in that enclosure impairs the appropriate production of the front chamber volume. To investigate the front chamber volume effect, three distinct front enclosure volumes, namely, 0.1, 0.5cc and 1cc, were considered. The front chamber volume was determined to be a major factor affecting f_H, (Fig. 12). To explore how the front chamber volume affects f_H, the volumes of 0.1cc [f_H = 9 KHz], 0.5cc [f_H = 5.6 KHz] and 1cc [f_H = 4.5 KHz] were investigated. In the simulation, modifying the front chamber volume resulted in variations of the compliance front sound transmission. The simulated and experimental *SPL* curves derived for the three cases are plotted in Fig. 12. Both the simulated and experimental results showed that smaller front chamber volumes are preferable because they yielded broader smooth regions from 850 Hz to 10 KHz. However, the front chamber volume between the microspeaker and the port must have a minimal value if the diaphragm must vibrate freely.

In the case, whole distribution model got agreement with experiment in high frequency range, because the mode shape of diaphragm in high frequency components can be calculated by finite-element method. Based on the simulation and experiment, we found the physic symptom if front chamber is increased, the high frequency response will be influenced. Based on that,

https://doi.org/10.1017/jmech.2017.64 Published online by Cambridge University Press

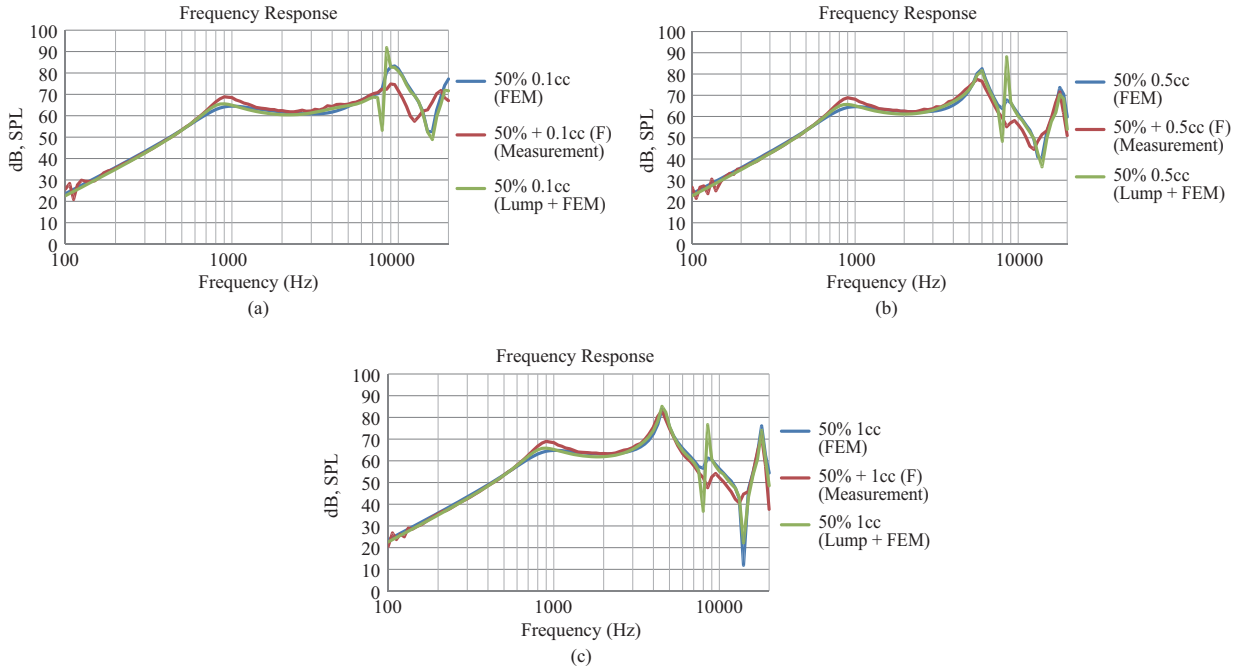


Fig. 12 Case 3 results, (a) 0.1cc front volume; (b) 0.5cc front volume; (c) 1cc front volume.

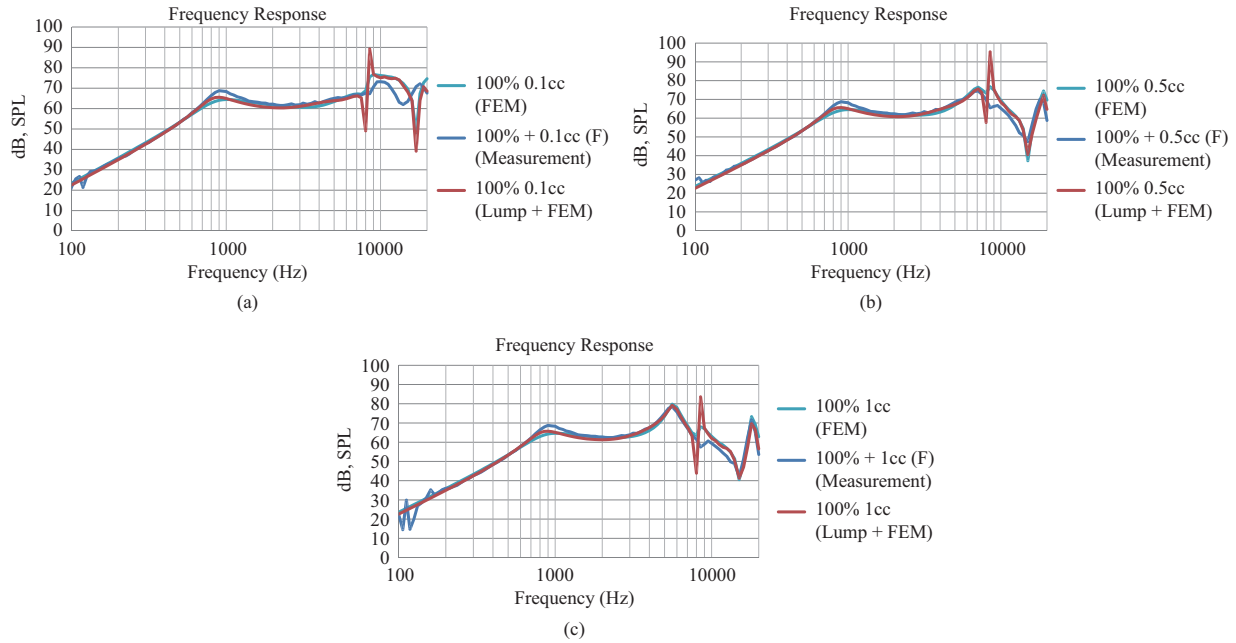


Fig. 13 Case 4 results, (a) 0.1cc front volume (b) 0.5cc front volume; (c) 1cc front volume.

small front chamber size is better and it will not affect high frequency response.

3.4 Case 4 Enclosures with 100% Open Areas with Different Front Chamber Volume

The case involving the 1cc back chamber volume shows that if an industrial design provides a 100% open rate for the sound port to reduce radiation impedance, then the placement of microspeaker within the enclosure impairs the appropriate production of the front chamber volume. To investigate the front chamber volume effect, three distinct front enclosure volumes, namely, 0.1, 0.5 and 1cc, were considered. The front chamber volume was determined to be a critical factor affecting its f_H, cases for 0.1cc [f_H = 10 KHz], 0.5cc [f_H = 7.1 KHz] and 1cc [f_H = 5.6 KHz] were investigated. In the simulation, modifying the front chamber volume resulted in variations of the compliance front sound transmission. The simulated and experimental *SPL* curves derived for the four cases, are plotted in Fig. 13. Both the simulated and experimental results show that smaller front chamber

https://doi.org/10.1017/jmech.2017.64 Published online by Cambridge University Press

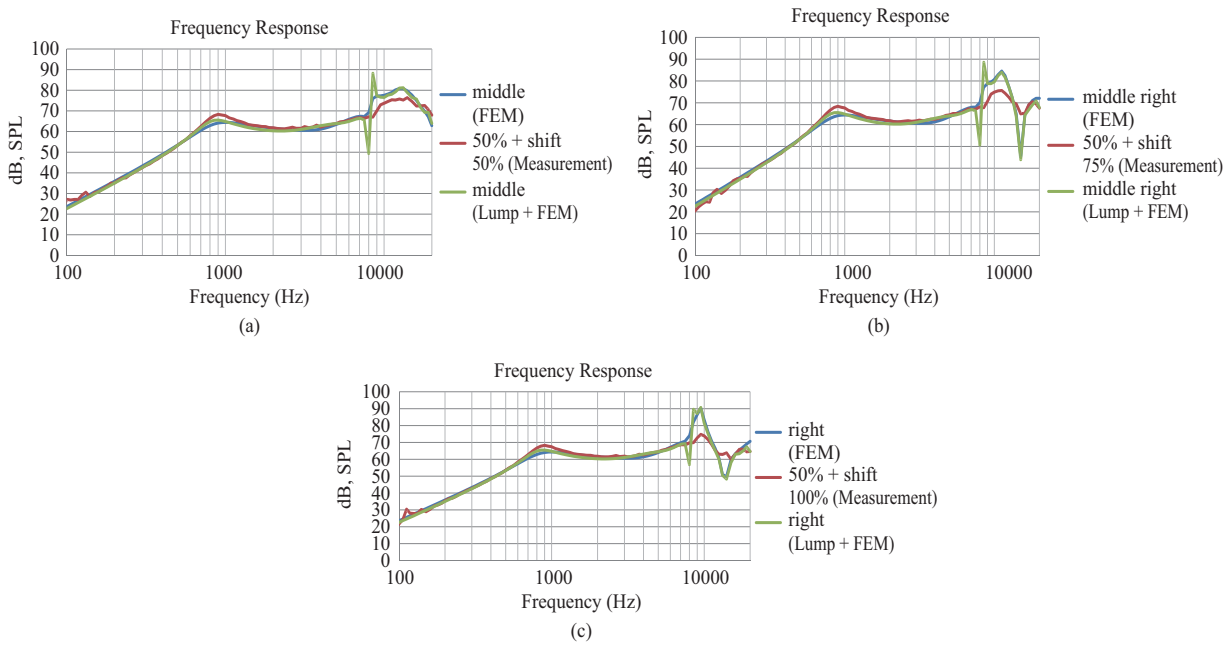


Fig. 14 Case 5 results, (a) shift 50%; (b) shift 75%; (c) shift 100%.

volumes are preferable because they produce broader smooth regions from 850 Hz to 10 KHz. However, the front chamber volume between the microspeaker and the port must have a minimal value if the diaphragm is to vibrate freely. In the case, whole distribution model got agreement with experiment in high frequency range, because the mode shape of diaphragm in high frequency components can be calculated by finite-element method. Comparison of case 3 and case 4, we found the physic symptom if front chamber is the same and open rate is increased, the high frequency response will be extended. Based on that, small front chamber size and large open rate are better and it will not affect high frequency response.

3.5 Case 5 Enclosures with 50% Open Areas with Shifted Holes

In practice, most ports are not located at the center of diaphragm because design constraints and the placement of required internal components limit product designs. In the simulation, sound-ports in various locations shifted the sound directivities in terms of the axial acoustic pressure. For three cases, *SPL* curves obtained from hybrid simulations and experimental results are plotted in Fig. 14. Both the simulations and experimental results show that shifted sound-port locations can influence high-frequency components higher than 10 KHz. The high-frequency components affect the sound transmission capability because designers prefer to apply ultrasonic components.

In the case, whole distribution model got agreement with experiment in high frequency range, because the mode shape of diaphragm in high frequency components can be calculated by finite-element method. Based on the simulation and experiment, we found the physic symptom if open hole is shifted, the high frequency response will not be influenced.

3.6 Case 6 Effect of Side-Firing

In this case, a plastic mobile enclosure, shown in Table 3 was considered. A small cavity at the front of the microspeaker system can be modeled as an acoustical compliance. The port at the small cavity results in acoustic resistance and mass. The duct was modeled using the aforementioned finite element model. The area of the duct exit was smaller than the cross-sectional area of the duct, creating an acoustic compliance effect. The effect of the port created acoustic resistance and mass, coupled with radiation impedance at the opening. Another resonance is presented in Fig. 15 at 3.5 KHz at a duct length of 10 mm. when the duct length was 5 mm, the high-frequency resonance was 5.3 KHz (Fig. 15). A duct height of 1 mm or 2 mm affected only the sound pressure level.

4. CONCLUSIONS

A rigorous electroacoustic analysis, based on lumped model and a distribution model, was conducted to investigate the influence of enclosure parameters on microspeaker driver units in mobile devices. Special attention was paid to the modeling of microspeaker enclosures, especially six cases are frequently used in commercial mobile devices. The performance of the system was also evaluated numerically and experimentally. A detailed parametric discussion, although highly crucial for engineers, has yet to be addressed in the open literature. Therefore, to address this gap, the paper presents an extensive case study on f_B, f_H, *SPL* and its physic symptoms. The physic symptoms can be found in

https://doi.org/10.1017/jmech.2017.64 Published online by Cambridge University Press

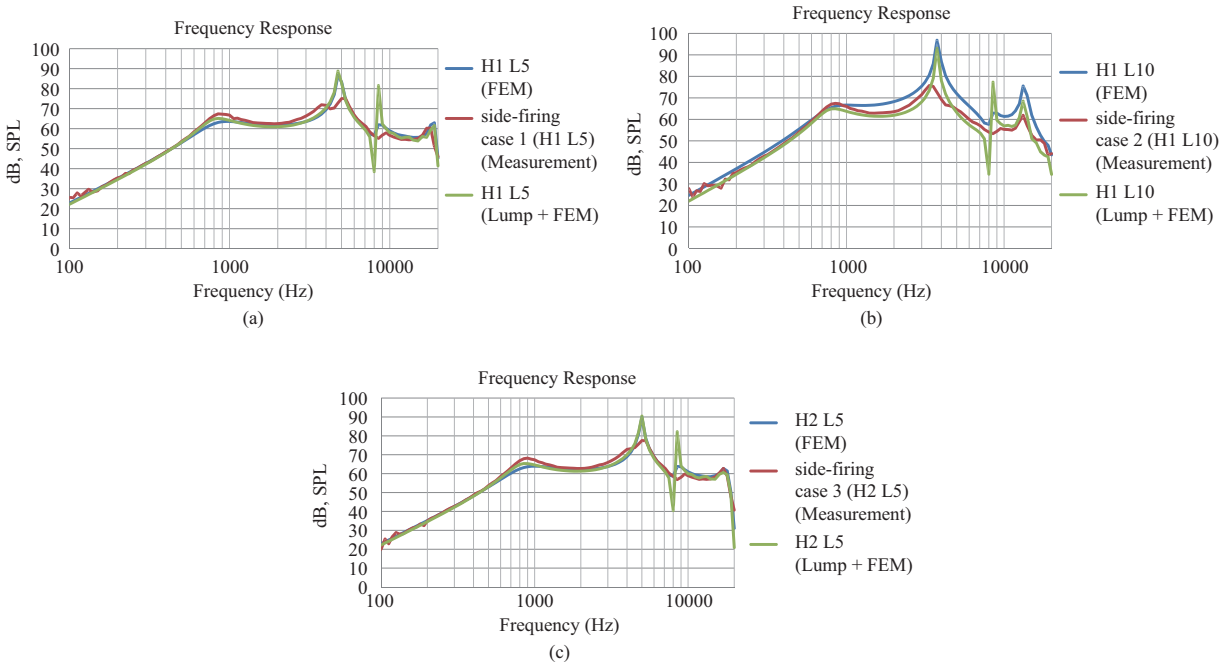


Fig. 15 Case 6 results, (a) H1 L5 case; (b) H1 L10 case; (c) H2 L5 case.

Table 4 Conclusion of enclosure design parameters.

	Enclosure Design Parameter	Parameters	Influence of System Performance
Case 1	Rear chamber volume	Big	Bass can be extended
		Small	Without bass effect
Case 2	Front open rate (1cc rear volume)	100%, 60%, 40%	Small open rate results in low value of f_H (high resonance frequency of enclosure)
Case 3	Front chamber volume (1cc rear volume and 50% open rate)	0.1cc, 0.5cc, 1cc	Small front chamber volume results in high value of f_H (high resonance frequency of enclosure can be extended)
Case 4	Front chamber volume (1cc rear volume and 100% open rate)	0.1cc, 0.5cc, 1cc	Small front chamber volume results in high value of f_H (high resonance frequency of enclosure can be extended) * compared to case 3, Results of f_H in case 4 are higher than case 3
Case 5	open hole location (1cc rear volume, 50% open rate)	In middle location, 50% shift, 100% shift	100% shift affects high frequency response
Case 6	Side-firing	channel length, channel height	Results of channel length affect high resonance frequency of enclosure, but channel height only affects *SPL*.

Table 4 to instruct the enclosure design parameters. By investigating each of these parameters, engineers in the 3C industry can optimize the *SPL* performance and frequency bandwidth of their basic microspeaker design concepts before executing designs.

ACKNOWLEDGEMENTS

The authors would like to thank the National Science Council of the Republic of China, Taiwan, for financially supporting this research under Contract No. NSC 101-2221-E-002-102.

REFERENCES

1. Siemens, E. W., "Improvement in Magneto-Electric Apparatus," *U.S. Patent No. 149,797* (1874).
2. Siemens, E. W., "Electromechanical 'Dynamic' or Moving-Coil Transducer," *German Patent No. 2355* (1877).
3. Rice, C. W. and Kellogg, E. W., "Notes on the Development of a New Type of Hornless Loudspeaker," *Journal of the Audio Engineering Society*,

https://doi.org/10.1017/jmech.2017.64 Published online by Cambridge University Press

er," *Journal of the Audio Engineering Society*, **30**, pp. 512-521 (1982).

4. Villchur, E. M., "Problems of Bass Reproduction in Loudspeakers," *Journal of the Audio Engineering Society*, **5**, pp. 122-126 (1957).
5. Villchur, E. M., "A Method of Testing Loudspeakers with Random Noise Input," *Journal of the Audio Engineering Society*, **10**, pp. 306-309 (1962).
6. Thiele, A. N., "Loudspeakers in Vented Boxes: Part 1," *Journal of the Audio Engineering Society*, **19**, pp. 382-392 (1971).
7. Thiele, A. N., "Loudspeakers in Vented Boxes: Part 2," *Journal of the Audio Engineering Society*, **19**, pp. 471-483 (1971).
8. Small, R., "Direct Radiator Loudspeaker System Analysis," *Journal of the Audio Engineering Society*, **20**, pp. 383-395 (1972).
9. Small, R., "Closed-Box Loudspeaker Systems-Part 1: Analysis," *Journal of the Audio Engineering Society*, **20**, pp. 798-808 (1972).
10. Small, R., "Closed-Box Loudspeaker Systems-Part 2: Synthesis," *Journal of the Audio Engineering Society*, **21**, pp. 11-18 (1973).
11. Small, R., "Vented-Box Loudspeaker Systems-Part 1: Small-Signal Analysis," *Journal of the Audio Engineering Society*, **21**, pp. 363-372 (1973).
12. Small, R., "Vented-Box Loudspeaker Systems-Part 2: Large-Signal Analysis," *Journal of the Audio Engineering Society*, **21**, pp. 438-444 (1973).
13. Small, R., "Vented-Box Loudspeaker Systems-Part 3: Synthesis," *Journal of the Audio Engineering Society*, **21**, pp. 549-554 (1973).
14. Small, R., "Vented-Box Loudspeaker Systems-Part 4: Appendices," *Journal of the Audio Engineering Society*, **21**, pp. 635-639 (1973).
15. Bai, M. R. and Liao, J., "Acoustic Analysis and Design of Miniature Loudspeakers for Mobile Phones," *Journal of the Audio Engineering Society*, **53**, pp. 1061-1076 (2005).
16. Bai, M. R. and Chen, R. L., "Optimal Design of Loudspeaker Systems Based on Sequential Quadratic Programming (SQP)," *Journal of the Audio Engineering Society*, **55**, pp. 44-54 (2007).
17. Bai, M. R., Liu, C. Y. and Chen, R. L., "Optimization of Microspeaker Diaphragm Pattern Using Combined Finite Element–Lumped Parameter Models," *IEEE Transactions on Magnetics*, **44**, pp. 2049-2057 (2008).
18. Shiah, Y. C., Her, H. C., Huang, J. H. and Huang, B., "Parametric Analysis for a Miniature Loudspeaker Used in Cellular Phones," *Journal of Applied Physics*, **104**, 104905 (2008).

(Manuscript received September 2, 2016, accepted for publication July 24, 2017.)

https://doi.org/10.1017/jmech.2017.64 Published online by Cambridge University Press